HYDROLOGICAL PROCESSES
Hydrol. Process. **18**, 3119–3132 (2004)
Published online in Wiley InterScience (www.interscience.wiley.com). DOI: 10.1002/hyp.5752

Application of a distributed hydrological model and weather radar observations for flood management in the upper Tone River of Japan

Dawen Yang,* Toshio Koike and Hiroshi Tanizawa
Department of Civil Engineering, University of Tokyo, Bunkyo-ku, Tokyo 113-8656, Japan

Abstract:

Through utilizing weather radar measurements, the present research explores the possibility of applying a coupled distributed hydrological model with reservoir operations to flood forecasting and control in the Okutone basin, located in the upstream region of the Tone River. The Tone River basin often suffers from heavy rainfall events as a result of rainy season frontal activity, typhoons and cumulus cloud activity associated with the local circulation. The reservoirs located in the Okutone basin play an important role in flood regulation. The simulation of a flood event in August 2001 shows the potential applicability of the distributed hydrological model and weather radar measurements for real-time flood control. Copyright © 2004 John Wiley & Sons, Ltd.

KEY WORDS Tone River; flood control; reservoir operation; distributed hydrological model; radar rainfall

INTRODUCTION

In present practical applications, lumped models are commonly employed for flood control and water resources management. Lumped models use averages of meteorological inputs and watershed characteristics in hydrological simulations and cannot directly use spatial information such as precipitation over the simulated catchment. Many studies address the calculation of the area-mean precipitation for the lumped model (Finnerty *et al*., 1997; Cranmer *et al*., 2001). However, the use of the area-average rainfall may introduce additional uncertainty during the process of estimating the basin-average rainfall. This also affects the hydrological simulation.

On the other hand, distributed models incorporate the temporal and spatial variability of catchment conditions and meteorological inputs and allow for a better representation of the hydrological processes than other model types (Yang *et al*., 2002). Developments in distributed hydrological models emphasize the capturing of the local unique contributions due to different land cover, soil properties and topography (Yang *et al*., 2001a). The importance of the spatial variability of precipitation using the distributed hydrological modelling approach has not been fully investigated, due to a lack of precipitation data of high spatial resolution. In recent literature, several studies have evaluated the performance of distributed hydrological models when utilizing spatially distributed precipitation (Cranmer *et al*., 2001; Taschner *et al*., 2001; Andersen *et al*., 2002; Yang *et al*., 2003a). The incorporation of distributed inputs of precipitation is expected to improve the simulation of hydrographs, but some results show no significant improvement. Yang *et al*. (2003a) compare hydrological simulations from a distributed model using gauge and radar rainfalls in the upper Tone River basin in Japan. The use of gauge rainfall results in a better estimation of long-term (no snowfall season)

* Correspondence to: Dawen Yang, Department of Hydraulic Engineering, Tsinghua University, Beijing 100084, China.
E-mail: yangdw@tsinghua.edu.cn

Received 25 June 2003
Accepted 26 March 2004

water balance, compared with the use of radar rainfall. However, better simulations of flood hydrographs are obtained using distributed radar rainfall patterns, compared with using the catchment-mean rainfall.

In addition to the commonly used rain gauge, weather radar and numerical weather-prediction models offer an opportunity to the hydrology community to improve flood forecasting and the prediction of water resources utilizing a distributed hydrological modelling approach. Nowadays, operational weather radars cover most of the land area in Japan and the interpreted precipitation information from radar measurements is available from several sources. The accuracy of radar-interpreted rainfall has improved significantly, especially as a result of the introduction of the dynamic window method (Yoshino, 2002).

The main objective of the present study is to identify the effect that including the spatial distribution of rainfall has on flood response, and to examine the applicability of the coupled distributed hydrological model with reservoir operation for flood control.

STUDY AREA

The Tone River is located northeast of Tokyo, Japan. The Okutone basin, which has been selected as the study area, is located in the high steep mountainous region of the upper Tone River (Figure 1). The elevation varies from about 300 m to 2600 m. The long-term mean precipitation in this region is about 1500 mm per year. This region usually experiences heavy snowfall during the winter (December to February) and experiences several typhoons during the late summer (August and September). Snowmelt runoff is the major water resource used for supplying Tokyo; however, Tokyo's high flood risk is as a result of typhoons. The catchment area of the Okutone basin lying upstream of the Iwamoto hydrological station is 1700 km^2. There are five reservoirs located in this basin (see Figure 1), which play an important role in flood regulation for protecting the Lower Kanto plain. Table I shows the main characteristics of the five reservoirs.

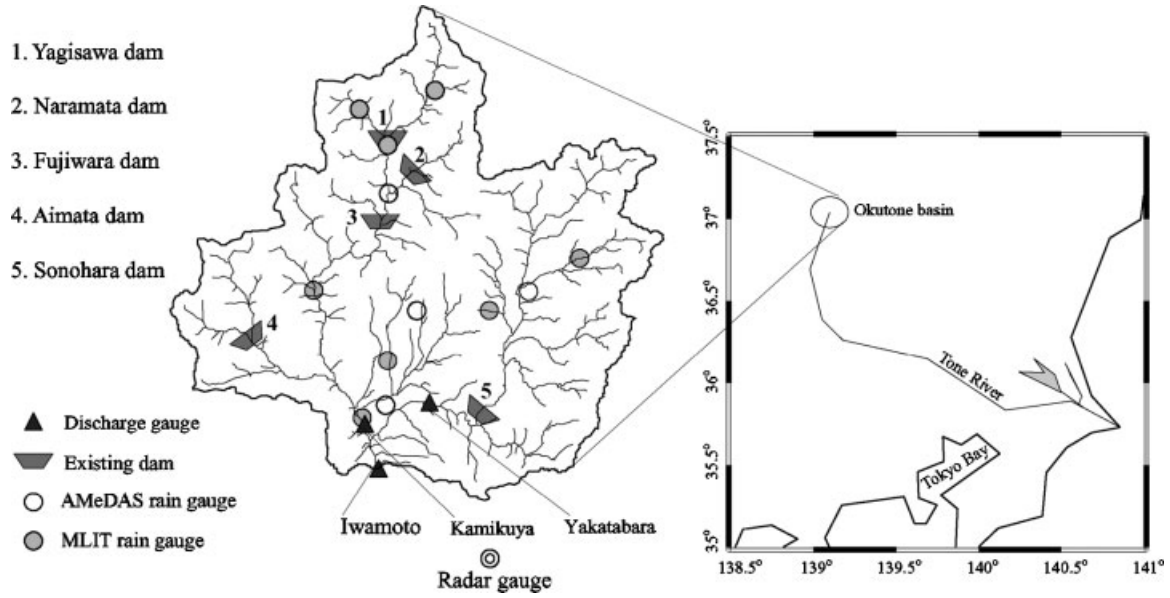

Figure 1. Study area

Table I. Characteristics of reservoirs located in the Okutone basin

Code in Figure 1	Name	Complete year	Drainage area (km^2)	Crest depth (m)	Total capacity (Mm^3)
1	Yagisawa	1967	167·4	131·0	204·3
2	Naramata	1990	60·1	158·0	90·0
3	Fujiwara	1958	401·0	95·0	90·0
4	Aimata	1958	110·8	67·0	25·0
5	Sonohara	1966	493·9	76·5	20·31

METHODOLOGY

The development of a distributed hydrological model starts with the collection of digital geographical information related to the study area for building a digital representation of the basin. This is the basis for making a distributed hydrological model. A digital elevation model (DEM) is used to define the target area, and the target basin is subdivided into a number of fundamental units for hydrological simulation. The catchment parameters related to topography, land use and soil are then calculated for each simulation unit. As shown in Figure 2, geographical information defines the general structure of the hydrological model. The study basin is divided into a discrete grid system, and the grid is represented by a number of geometrically symmetrical hillslopes. The river network is divided into subcatchments of an appropriate size. Dam locations are defined in the river network. The components of the hydrological model include the data input, the hydrological simulation and the resulting output. The hydrological simulation part includes runoff generation from the hillslope and the flow routing in the river network. The reservoir operation is coupled with the river flow routing.

Data preparation

Geographic information system data. The geographical information used for the construction of a distributed hydrological model includes the topography, the land cover, the soil, and geological maps. The digital data of

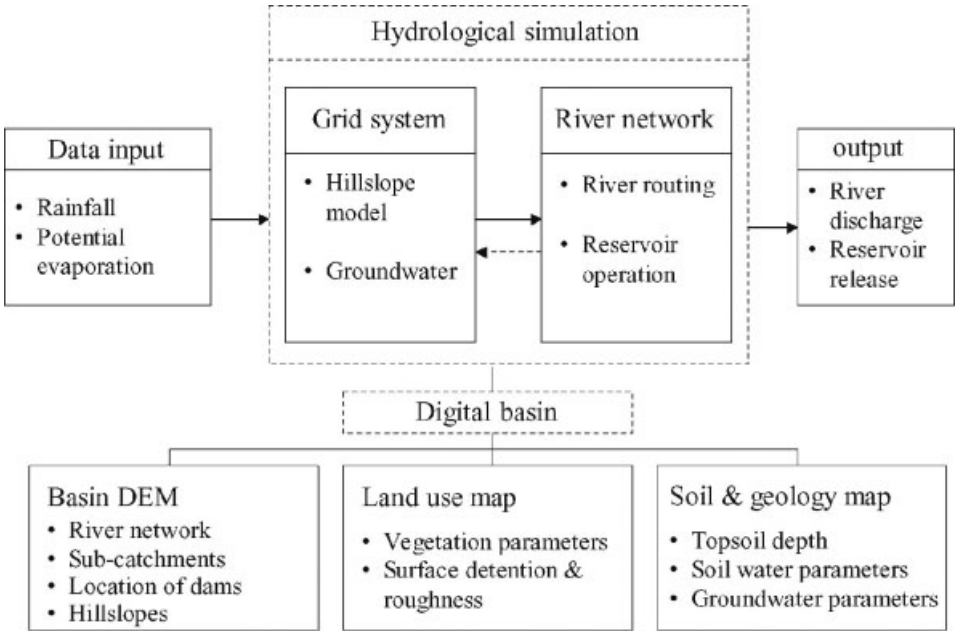

Figure 2. General structure of the hydrological model

elevation, land use and geological conditions were obtained from the Japan Geographical Survey Institute. The topography is simulated using a grid-based DEM with the available finest resolution of 50 m. All topographical parameters are calculated from the 50 m DEM. A digital land-use map is available at a 100 m resolution, and has been grouped into five categories: forest (85%), grassland (7·5%), bare soil covered by sparse grass (5%), built-up land (1%), cropland (1%); the water body makes up the remainder (0·5%).

In the global digital soil map (FAO, 2003), which has 5′ longitude/latitude resolution, the effective soil depth is classified into six groups: <10 cm, 10–50 cm, 50–100 cm, 100–150 cm, 150–300 cm, and >300 cm. Through combination with the geological map provided by the Japan Geographical Survey Institute, the topsoil depth has been estimated to range from 1 to 5 m, with depths of around 1–2 m in most areas. The distribution of the topsoil type is obtained from a 1000 m resolution soil map. According to the permeability, the topsoil is classified into four types (see Table II). Basically, the soils belong to the Kanto loam category, and their soil water parameters, except for the saturated hydraulic conductivity, are treated uniformly. The vertical distribution of the saturated hydraulic conductivity of the topsoil is assumed to decrease exponentially from K_0 near the soil surface to K_g for groundwater at the bottom of the topsoil. K_0 and K_g are parameters that require calibration. Table II shows the soil-water parameters used in the hydrological simulations.

Precipitation. The gauge data are available from the Automated Meteorological Data Acquisition System (AMeDAS) provided by the Japanese Meteorological Agency (JMA), the Ministry of Land, Infrastructure and Transportation (MLIT), and the Japan Water Agency. These data sources are available at 1 h resolution. A few of the AMeDAS gauges measure four parameters: precipitation, temperature, wind speed, and sunshine duration. The availability of meteorological gauges in the Okutone basin is shown in Figure 1. Thiessen polygons are used for estimating the distribution of rainfall from point measurements.

This study uses rainfall results interpreted from radar measurements directly, which have been provided by the Foundation of Rivers & Basin Integrated Communications (FRICS) of Japan. These data are available at 5′ temporal and 1 km spatial resolutions from 2001. The flood event of 22 August 2001 is selected for this study according to the availability of precipitation data from both gauges and radar measurements.

The distributed hydrological model

In order to use radar rainfall, a grid-based distributed hydrological model is used in this study, which is modified from the geomorphology-based hydrological model (GBHM) (Yang *et al.*, 2002). As mentioned

Table II. Soil parameters used in the hydrological model

Soil type	High-permeability soil	Black soil	Forest soil	Red soil
Coverage (%)	15	22	56	7
Saturated hydraulic conductivity of topsoil K_0 (mm h^{-1})	80·0	25·0	50·0	60·0
Hydraulic conductivity of groundwater K_g (mm h^{-1})		1.0		
Saturated volumetric moisture content of topsoil θ_s		0.51		
Residual volumetric moisture content of topsoil θ_r		0.17		
Parameter for soil water retention curve and hydraulic conductivity in the Van Genuchten's (1980) equation (unit of matric pressure: cm water)		$a = 0.017$ $n = 1.413$		

above, the finest DEM is available at 50 m spatial resolution. In order to represent the topography accurately, the hydrological model should also use the same grid size. Unfortunately, grid-based distributed hydrological models usually cannot run at high spatial resolution for practical applications due to their heavy computational requirement. A realistic resolution is required for producing a discrete catchment on which the hydrological simulation can be carried out. Aggregation from a fine DEM to a coarse DEM decreases the gradient and increases the length of the hillslope. Besides the topography, the heterogeneity of the vegetation and soil within computational grids also needs to be considered. Therefore, a subgrid parameterization scheme is necessary when a hydrological model uses a large-sized computational grid. However, the soil type is treated as uniform within grids due to the spatial resolution of the soil data.

Subgrid parameterization. In this study, the grid size in the hydrological model is 500 m. The spatial heterogeneity inside a 500 m grid is considered in the hydrological model. Figure 3 shows the concept of the subgrid parameterization used in the grid-based distributed hydrological model. The distinguishing characteristic of the methodology on the subgrid parameterization is the representation of the subgrid variability of topography in terms of geomorphological properties. In the GBHM developed by Yang *et al*. (2002), the geomorphological property of the river–hillslope formation is used to represent the catchment topography. In a similar way, it is assumed that a large grid is comprised of a set of hillslopes located along the streams. Within a computational grid, all hillslopes are viewed as being geometrically similar. A hillslope of unit width is called a hillslope element, which is represented by a rectangular inclined plane (Figure 3). The length of a hillslope element is calculated from the 50 m DEM as

$$l = a(i, j)/2 \sum L \tag{1}$$

where $a(i, j)$ is the area of the grid at location (i, j), which is 0·25 km^2 here, but can also be a variable area if it is in a geographic (longitude/latitude) coordinate system; $\sum L$ is the total length of streams extracted from the 50 m DEM. The slope angle is taken to be the mean slope of all subgrids in the 50 m DEM. The impermeable bedrock slope is assumed to be parallel to the surface.

Considering the subgrid heterogeneity of vegetation, the hillslopes within a computational grid are grouped into different vegetation categories. The area fraction of each uniform vegetation class is calculated from the land-use map. Therefore, the fundamental unit for the hydrological simulation is the hillslope with uniform soil and vegetation types. The hydrological response from a computational grid is the total of the responses from all hillslopes within the same grid. The streams located inside a grid (see Figure 3) are lumped into a single channel which flows along the main flow direction of this grid. The hydrological responses from hillslopes are assumed to distribute uniformly along the single lumped channel. In the discrete computational grid system of a study catchment, the river network links all of the grids, and the catchment hydrological response is obtained by solving flow routing in the river network.

Hillslope hydrological model. A physically based model is used to simulate the hydrological response from hillslopes. The hydrological processes included in this model are the canopy interception, evapotranspiration, infiltration, surface flow, subsurface flow and the exchange between groundwater and the river (Yang *et al*., 2002). The canopy interception ability S_{C0} is described using a linear function of the leaf-area index (LAI; Sellers *et al*., 1996) as

$$S_{C0}(\text{mm}) = 0{\cdot}2\text{LAI} \tag{2}$$

The LAI differs between vegetation species. The actual interception is determined by the rainfall intensity and deficit of the canopy storage (Yang *et al*., 2002). Water can evaporate from the canopy-intercepted water and soil surface, and can transpire by vegetation taken from the root zone. The actual evapotranspiration is estimated from the potential evaporation. The potential evaporation is estimated using temperature, wind speed and sunshine hours from the AMeDAS data.

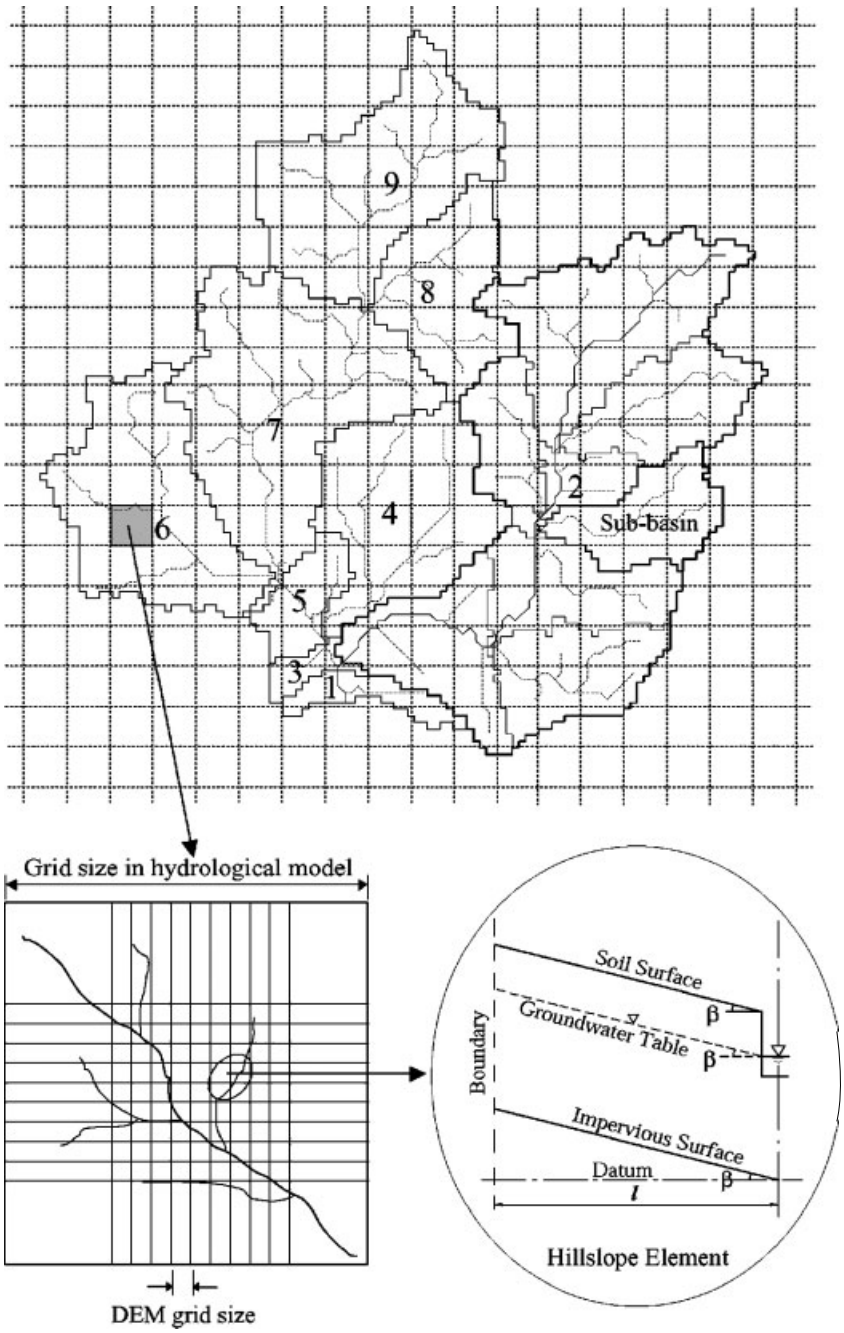

Figure 3. Concept of the grid-based hydrological model

The infiltration and water flow in the subsurface in the vertical direction and along the hillslope are described in the quasi-two-dimensional subsurface model. The vertical water flow in the topsoil is represented by the Richards equation and solved by an implicit numerical solution scheme. In this scheme, the topsoil is divided into multiple layers. The depth of the first layer is 5 cm, and the remaining layers increase in depth to two

times that of the upper layer, which must be less than the maximum of 50 cm. The first layer is assumed to be saturated throughout the rainfall period. Therefore, the upper boundary condition is given as the saturation of soil moisture for the rainfall cases. During non-rainfall periods, the upper boundary condition is given as the evaporation flux. The transpiration flux is treated as a sink in the soil layers within the root zone. The lower boundary condition is given as saturated because the groundwater reaches very high levels during the flood season. The precipitation and hydrological characteristics along the hillslope are uniform in the present model. The soil water distribution along the hillslope is treated as uniform. The depth of the surface water due to infiltration and saturation excess is calculated by solving for the vertical one-dimensional soil water movement using the Richards equation, and the precipitation is distributed uniformly along the hillslope. In the subsurface of the topsoil, the soil water moves due to gravity along the hillslope towards the stream when the moisture content is more than the field capacity. The subsurface flow process is described by

$$q_{\text{sub}} = K(\theta) \sin \beta \tag{3}$$

where q_{sub} is the flow rate, $K(\theta)$ is the hydraulic conductivity and β is the slope. The soil water content θ should be larger than the field capacity in this case.

The surface runoff is the discharge that flows through the hillslope into the stream, which is treated as sheet flow and solved using Manning's equation. Groundwater aquifers are treated as individual storages corresponding to each grid. The exchange between the groundwater and the river water is considered as steady flow and is calculated using Darcy's law (Yang *et al*., 2002).

The runoff generated from a grid is the sum of the hillslope responses, including both the surface and subsurface runoff. State variables, such as the soil moisture content of a grid, are output as the average value for the grid. The vertical flux, the actual evapotranspiration of a grid, is the total flux simulated from all hillslopes in the same grid.

Flow routing in the river network. In order to simulate flow routing in the river network, the number of river segments (links) and the flow sequences need to be defined. Here, the Pfafstetter scheme (Yang *et al*., 2000; Yang and Musiake, 2003b) is applied for subdividing the catchment and for numbering the flow sequences among the subcatchments. The catchment is divided into nine subcatchments systematically using this scheme. If a subcatchment is still sufficiently large, then it is subdivided again using the same method. By repeating the same procedure, the catchment is finally divided into a number of subcatchments with a limited drainage area. The drainage area of the subcatchment that is divided using the Pfafstetter scheme depends on the requirement of the hydrological simulation and the DEM resolution. In the present study of the Okutone basin, the average drainage area of the subcatchment is about 10 km^2.

As mentioned above, streams located in a single grid are lumped into a single channel. It is practically difficult to identify and represent all of the river channels in a grid-based hydrological model. Therefore, the river networks of a subcatchment are simplified such that only the main river is considered. The lateral inflow into the main river is the total runoff generated from all of the grids at the same flow distance in the same subcatchment. The flow sequences among these simplified main rivers are defined by the codes of the divided subcatchments. The flow routing of all the river networks in the catchment is modelled using the kinematic wave approach.

Reservoir operation

Reservoir operations are commonly modelled using the storage approach for hydrological applications. The basic equation is given by

$$\frac{\mathrm{d}V}{\mathrm{d}t} = Q_{\text{in}} - Q_{\text{out}} \tag{4}$$

where Q_{in} is the inflow, Q_{out} is the outflow, and V is the storage. Once the inflow, initial conditions, reservoir characteristics (e.g. relationship between the water level and volume/storage, i.e. H–V curve, H = water

level, V = volume/storage), and the operational rules are known, the outflow from a reservoir can be simulated (Ponce, 1989). The operational rule is usually designed according to the reservoir capacity, the inflow condition, and the downstream needs. For the long-term mean, the reservoir water level changes regularly throughout a hydrological year. The long-term mean water level can be used as the operational rule for simulating reservoir release. But in using an operational curve represented by the mean water level, a simulation can only capture the mean value of reservoir release in a large time step, which is insufficient for flood regulation (Yang *et al*., 2001b).

The simplest form of the above finite difference equation is

$$\frac{V_2 - V_1}{\Delta t} = \frac{Q_{\text{in}}^1 + Q_{\text{in}}^2}{2} - \frac{Q_{\text{out}}^1 + Q_{\text{out}}^2}{2} \tag{5}$$

where the index '1' indicates the current time level, '2' indicates the next time level, and Δt is the time interval. The reservoir release for the period between time levels 1 and 2 is viewed as being constant and is given as Q_{out}^1. Thus, the reservoir storage at time level 2 is obtained using

$$V_2 = V_1 + \left(\frac{Q_{\text{in}}^1 + Q_{\text{in}}^2}{2} - Q_{\text{out}}^1 \right) \Delta t \tag{6}$$

The inflows are calculated from hydrological simulations and the storage V_2 can be calculated using Equation (6). The reservoir release Q_{out}^2 for the next time step is then determined according to the operational rule. Figure 4 shows the flowchart for the reservoir operation.

During a flood period, reservoirs are operated manually. The reservoir release discharge is determined according to the present water level of the reservoir, the inflow discharge into the reservoir and the water use requirement (MOC, 1995). For dam safety, the upper limit of the water level is defined during the design stage as the flood warning level. When the water level exceeds the warning level, water is released from the spillways and the discharge is determined by the structure type of the spillway and the hydraulic conditions. Each reservoir has its own operational rule, independent of other reservoirs.

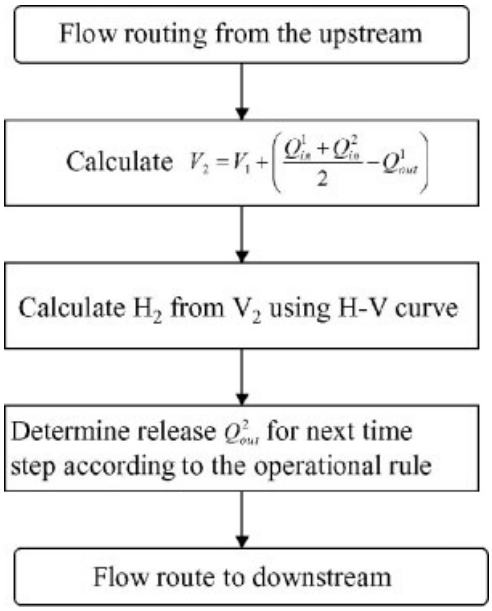

Figure 4. Flowchart for determining reservoir release

In an extreme case, a reservoir is operated according to the judgment of the director of the reservoir operation office, which is determined through consideration of the state of the reservoir and the downstream flood conditions. Here, the normal operation rule for each reservoir of the Okutone basin is included in the hydrological model.

MODEL APPLICATION, RESULT AND DISCUSSION

In this application, the model runs from 1 to 31 August 2001 using a 1 h resolution, and the results are examined for a 72 h period centred at the peak of the flood. There are two main tasks in this application: (1) to validate the efficiency of the model using radar rainfall for flood forecasting; (2) to validate the applicability of the coupled model considering reservoir operation and distributed hydrological simulation.

In order to specify the appropriate initial conditions for soil moisture and groundwater, the model is run for a period of 1 month prior to the flood event. The model parameters, i.e. the saturated hydraulic conductivity of the first layer near the soil surface and the hydraulic conductivity of the groundwater, are calibrated using the Aimata basin, and are then transferred to the whole of the study area (see Table II).

Efficiency of radar rainfall for flood forecasting

For the first task, simulations of inflows to four reservoirs in the uppermost stream, i.e. the Yagisawa, Naramata, Aimata and Sonohara, are examined. Figure 5a–d compares the simulated results using both gauge and radar rainfall inputs. In the Yagisawa subcatchment, the hydrograph simulated using gauge rainfall is more accurate than the hydrograph simulated using radar rainfall. In the other three subcatchments, however, the hydrographs simulated using radar rainfall are better than those simulated using gauge rainfall. The spatially averaged rainfall is illustrated above each hydrograph. The general patterns of rainfall are similar between gauge and radar data, but the differences between their simulated hydrographs are large. There are no rain gauges located inside the drainage basin of the Aimata dam, and the nearest gauge is very far from the centre of this sub-basin. In the drainage basin of the Sonohara dam, there are three rain gauges, but they are too close to each other and are concentrated in the middle of this basin. For the Aimata and Sonohara sub-basins, the simulated flood peaks from gauge rainfall are about two times higher than the observed.

The array of rain gauges is poor, as they are sparsely distributed and in many cases located in valleys. The situation becomes worse in the case where the rainfall field being observed is moving during a typhoon. In contrast, radars are able to measure the spatial patterns of rainfall better than rain gauges. From the above results, it can be seen that the spatial variability of rainfall is important for flood simulation. The accuracy of flood simulations can be greatly improved by utilizing radar measurements. However, the present algorithm for rainfall interpretation from radar measurements should also be improved for better estimates of rainfall values. As shown in Figure 5a, radar rainfall does not display a second peak, as shown by the actual hydrograph. This might have been caused by a mountain effect on the radar signal. Figure 6 shows the average rainfall over the drainage area of the Yagasawa dam measured using rain gauges and the radar. It can be seen that the rain gauges have measured rainfall after 16 : 00 on 22 August, which generated the second peak in Figure 5a. However, the radar measurement shows no rainfall during the same period.

Validation of the coupled distributed model with the reservoir operation

In the present combined model, the reservoir operation rule determines the release from a reservoir based on the inflow calculated using only the distributed hydrological model and the current water level. This type of operation rule is normally used in the Okutone basin during the flood season. The Yagisawa and Naramata reservoirs did not have any release to the downstream during the flood event, and the simulated results reflect that situation. Comparisons of the simulated and actual outflows from the Fujiwara, Aimata and Sonohara reservoirs are shown in Figure 7a. The simulated releases from the Aimata and Sonohara reservoirs are close

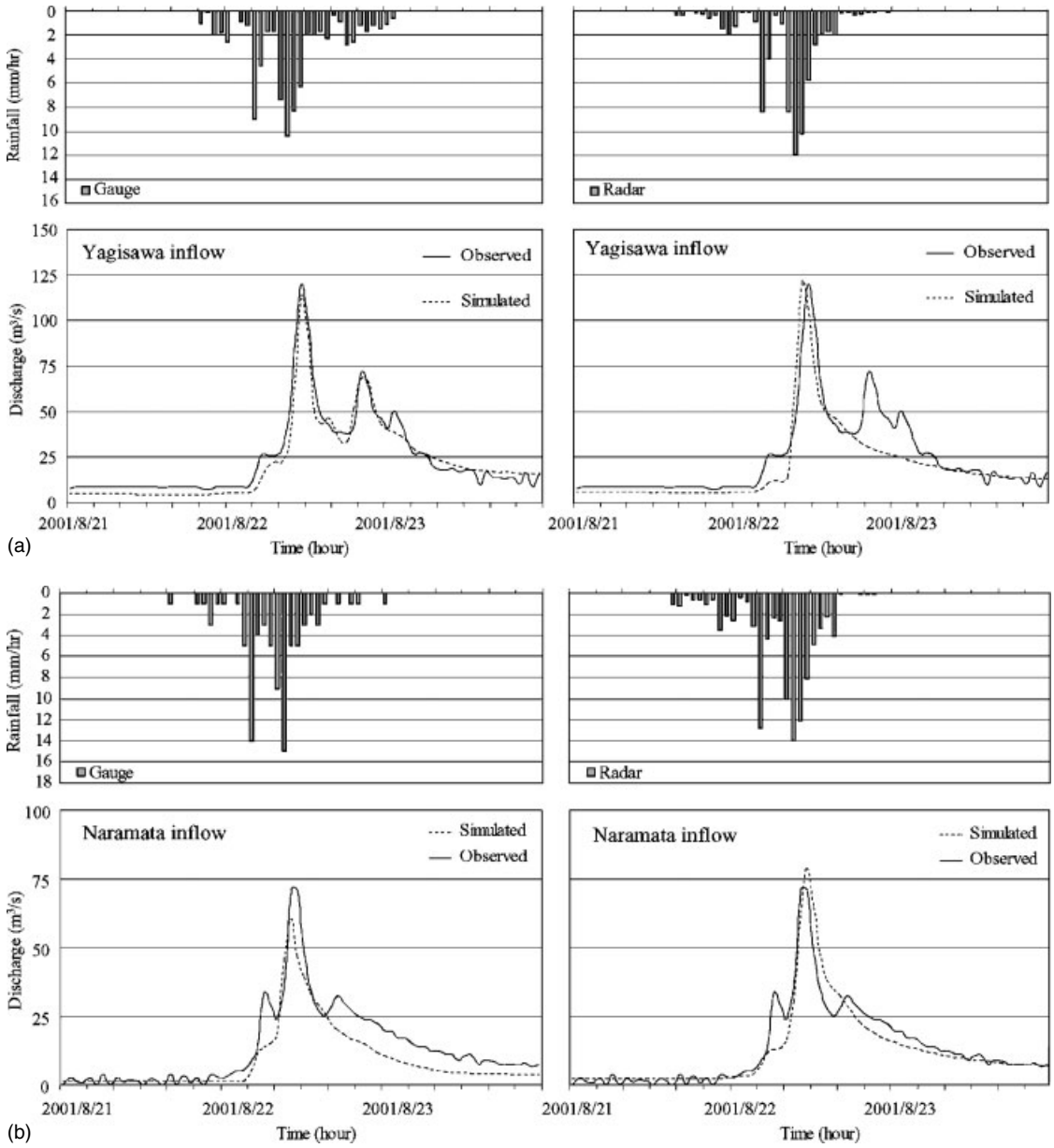

Figure 5a. Comparison of inflow simulations using different rainfall data: (a) Yagisawa reservoir; (b) Naramata reservoir; (c) Aimata reservoir; (d) Sonohara reservoir

to the actual releases, but the simulated release from the Fujiwara reservoir is much higher than the actual one. Releases from the Aimata and Sonohara reservoirs follow the free overflow, but the actual release from the Fujiwara reservoir remains constant during the flood event. This is the result of the special operation for regulating floods, which is performed by the reservoir manager. Disregarding the periods involving such special operations, this model can accurately simulate reservoir operations under normal situations.

Figure 7b shows the simulated hydrographs at three discharge gauges (see Figure 1). Generally, the coupled hydrological model with reservoir operation successfully mimics the actual hydrographs during the flood

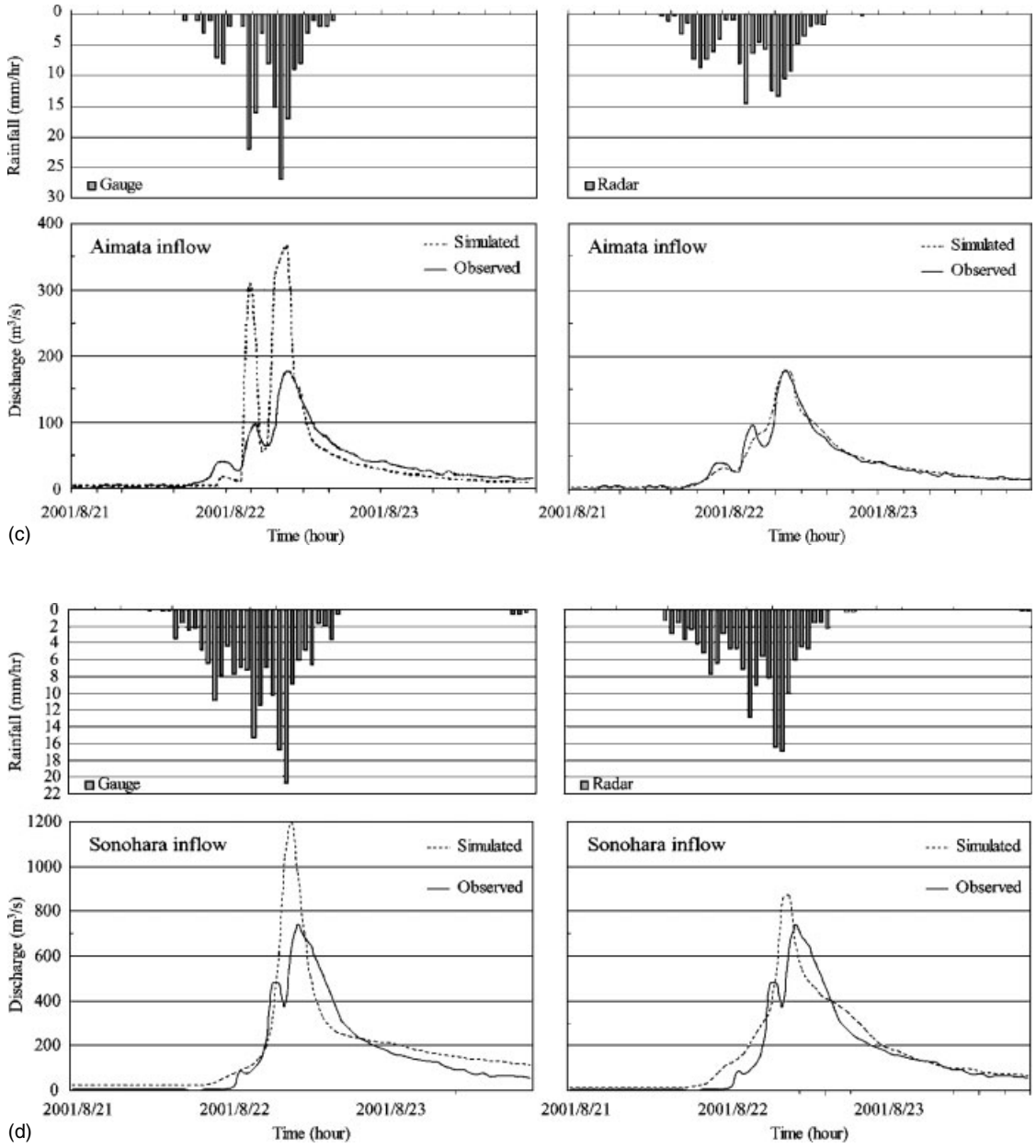

Figure 5b. (*Continued*)

event that occurred on 22 August 2001. But there is a 1 h time lag between the simulated and observed flood peaks, where the simulated peak occurs earlier than the actual peak. This might be caused by the flow routing in reservoirs, which involves reservoir lakes with narrow and long characteristics. The present simulation of reservoir operation uses a storage-based method without considering the reservoir flow routing. The hydrological model simulates the inflow discharge into the reservoir without considering the actual water level in the reservoir. This means that the downstream boundary condition used in the inflow simulation in the hydrological model is a free boundary. The kinematic wave method is also employed for flow routing.

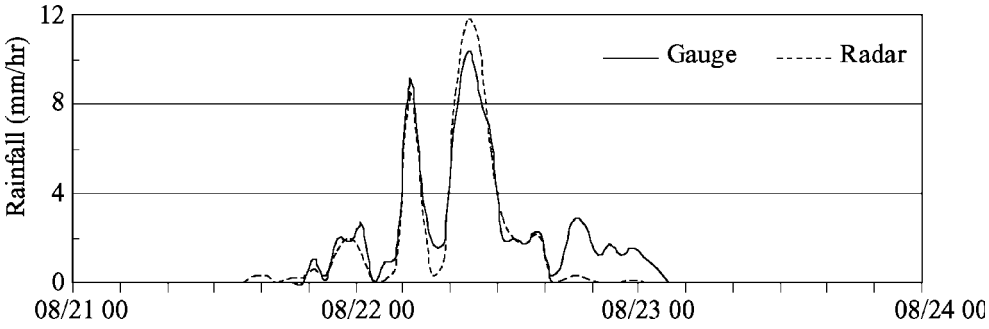

Figure 6. Comparison of the rainfalls over the Yagasawa dam drainage area measured using gauge and radar

Therefore, the high water level at the dam site and its backward effect on the inflow is not included in the present model. This is a deficiency that needs to be addressed in future model development. The dam effect on the delay of inflow may not be as long as 1 h in the Okutone basin, but the simulation uses a time step of 1 h. In future studies, the hydrological simulation should be carried out at time steps shorter than 1 h.

Discussion of the efficient operation of reservoirs for flood control

The Okutone basin contains two main tributaries on its west side, including the Sonohara reservoir, and another four reservoirs on its east side. The capacity of the Sonohara reservoir is the smallest in the Okutone basin, and it does not have sufficient flood control capability. The Yagisawa, Naramata and Fujiwara reservoirs have relatively larger capacities. It is possible to regulate flooding using only the Yagisawa, Naramata and Fujiwara reservoirs located on the east side. By checking the rainfall on 22 August 2001 illustrated in Figure 5a–d, it is found that the rainfall intensity in the Sonohara sub-basin is higher than on the other side. During the flood event, the water levels of the Yagisawa and Naramata reservoirs did not reach flood levels. Therefore, there were no releases from the two reservoirs. The Fujiwara reservoir carried out normal operation during the simulation. But in actuality, a special operation had been carried out for the Fujiwara reservoir in order to reduce the flood peak in the downstream region. However, the reduction in the flood peak was limited (see the simulated and actual releases from the Fujiwara reservoir shown in Figure 7a).

Supposing that the opposite spatial distribution of rainfall had occurred (the rainfall intensity in the Sonohara sub-basin was lower than on the other side), with the reservoir capacities for flood control located on the east side being larger than the Sonohara reservoir, the flood peak downstream would have been greatly reduced. However, when these reservoirs located on the east side use their flood control capacities, a request is made by the Sonohara reservoir for special operation. In this case, the flood cannot be reduced significantly further due to the very small capacity of the Sonohara reservoir.

For a more efficient control of floods it is necessary to introduce an integrated reservoir operation into the Okutone basin. For this integrated operation, the inflow needs to be forecast and the situations of other reservoirs and downstream flow conditions need to be considered. However, it is usually difficult to predict these conditions during emergency conditions. The present model demonstrates an ability to simulate inflows into reservoirs and the downstream flow conditions simultaneously using the coupled distributed hydrological model with reservoir operations. For real-time integrated flood management, it can provide a reference condition through the use of real-time rainfall measurements or rainfall forecasts. The present model is a useful tool for developing criteria for integrated reservoir operations in addition to normal operation rules, and can be used to investigate the efficiency of flood control under different conditions of spatial and temporal distributions of rainfall.

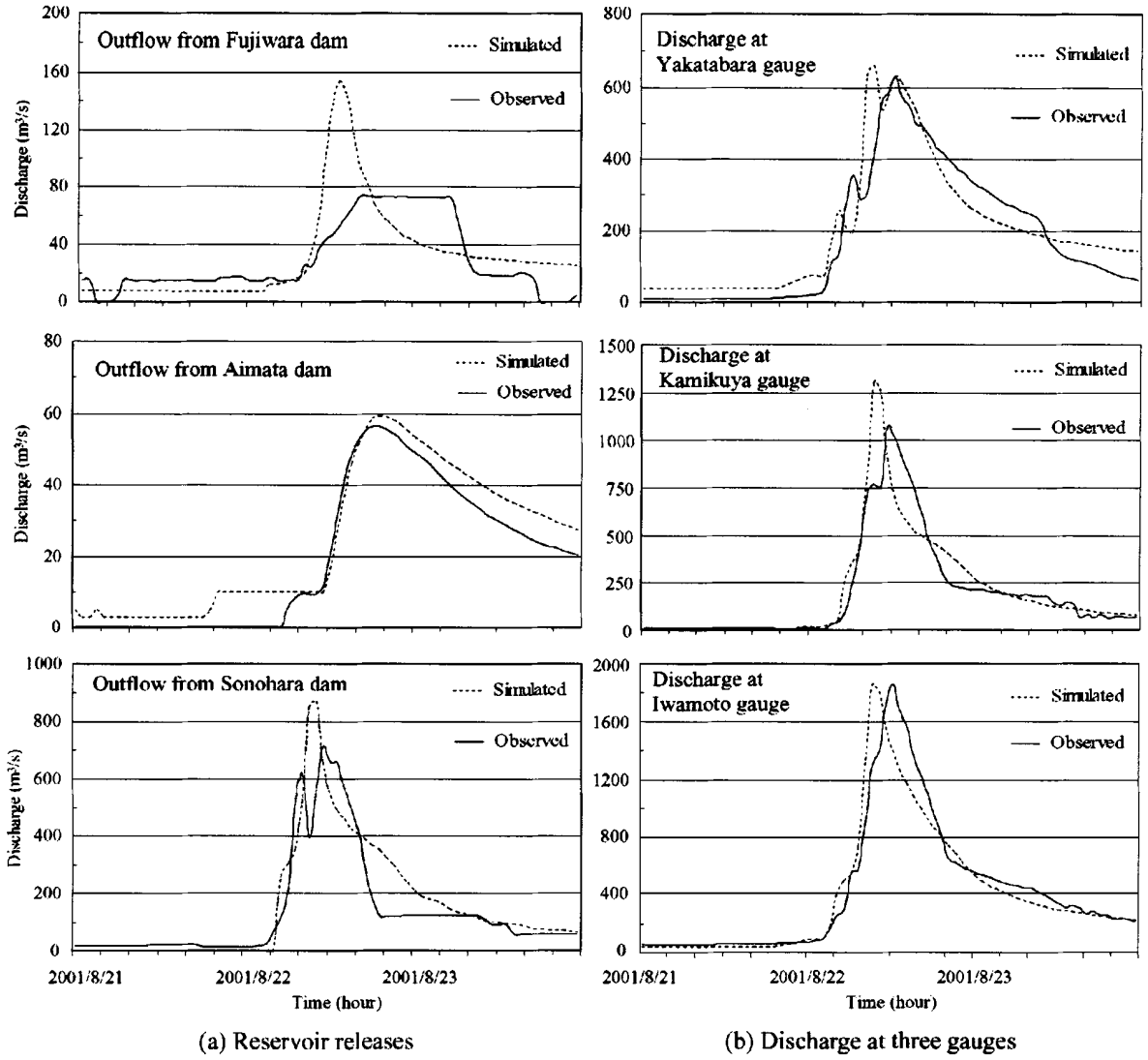

Figure 7. Simulations of reservoir releases and discharges at three gauges: (a) reservoir releases; (b) discharges at three gauges

CONCLUSIONS

A coupled distributed hydrological model considering reservoir operation has been developed and applied to the Okutone basin to investigate its applicability to flood control together with use of weather radar measurements. Through a comparison of gauge and radar rainfall on 22 August 2001 and their simulated flood hydrographs, it can be seen that radar measurements captured the spatial pattern of rainfall better than the rain gauges, and greatly improved the accuracy of the simulations of the inflows into the reservoirs. Simultaneously, the coupled model successfully simulated releases from the reservoirs in terms of the independent operational rule used in normal flood regulation. However, the high water level at the dam site and its backward effect on the inflow should be improved in future model development, as this has a significant effect on the timing of the peak in flood simulations.

In investigating the integrated reservoir operation for efficient flood control in the Okutone basin, this model serves as a useful tool for forecasting the inflow and the situations of all reservoirs and the downstream conditions simultaneously. This research demonstrated the advantages of using distributed hydrological and radar measurements in practical applications of flood management.

ACKNOWLEDGEMENTS

We would like to thank the Tonegawa Integrated Dam and Reservoir Group Management Office for providing the radar precipitation data required for this study.

REFERENCES

Andersen J, Dybkjaer G, Jensen KH, Refsgaard JC, Rasmussen K. 2002. Use of remotely sensed precipitation and leaf area index in a distributed hydrological model. *Journal of Hydrology* **264**: 34–50.

Cranmer AJ, Kouwen N, Mousavi SF. 2001. Proving WATFLOOD: modeling the nonlinearities of hydrologic response to storm intensities. *Canadian Journal of Civil Engineering* **28**: 837–855.

FAO. 2003. *Digital soil map of the world and derived soil properties*. Land and Water Digital Media Series Rev. 1, United Nations Food and Agriculture Organization, CD-ROM.

Finnerty BD, Smith MB, Seo DJ, Koren V, Moglen GE. 1997. Space–time scale sensitivity of the Sacramento model to radar-gage precipitation inputs. *Journal of Hydrology* **203**: 21–38.

MOC. 1995. *Reservoir operation manuals for the upper Tone River basin*. The Reservoir Management Office of the Upper Tone River Basin, Kanto Bureau, Ministry of Construction.

Ponce VM (ed.). 1989. *Engineering Hydrology: Principle and Practices*. Cambridge University Press/Prentice Hall; 1153pp.

Sellers PJ, Randall DA, Collantz GJ, Berry JA, Field CB, Dazlich DA, Zhang C, Collelo GD, Bounoua L. 1996. A revised land surface parameterization (SiB2) for atmospheric GCMs. Part I: model formulation. *Journal of Climate* **9**: 676–705.

Taschner S, Ludwig R, Mauser W. 2001. Multi-scenario flood modeling in a mountain watershed using data from a NWP model, rain radar and rain gauges. *Physics and Chemistry of the Earth, Part B: Hydrology, Oceans and Atmosphere* **26**: 509–515.

Van Genuchten M. 1980. A closed-form equation for predicting the hydraulic conductivity of unsaturated soil. *Soil Science Society of America Journal* **32**: 329–334.

Yang D, Musiake K, Kanae S, Oki T. 2000. Use of the Pfafstetter basin numbering system in hydrological modeling. In *Proceeding: Annual Conference of Japan Society of Hydrology and Water Resources*; 200–201.

Yang D, Herath S, Musiake K. 2001a. Spatial resolution sensitivity of catchment geomorphologic properties and the effect on hydrological simulation. *Hydrological Processes* **15**: 2085–2099.

Yang D, Herath S, Oki T, Musiake K. 2001b. Application of distributed hydrological model in Asian monsoon tropic region with a perspective of coupling with atmospheric models. *Journal of the Meteorological Society of Japan* **79**(1B): 373–385.

Yang D, Herath S, Musiake K. 2002. Hillslope-based hydrological model using catchment area and width functions. *Hydrological Sciences Journal* **47**(1): 49–65.

Yang D, Koike T, Tanizawa H. 2003a. Effect of precipitation spatial distribution on the hydrological response in the upper Tone River of Japan. In *Weather Radar Information and Distributed Hydrological Modelling*, Tachikawa Y, Vieux BE, Georgakakos KP, Nakakuta E (eds). IAHS publication No. 282. IAHS Press: Wallingford; 194–202.

Yang D, Musiake K. 2003b. A continental scale hydrological model using distributed approach and its application to Asia. *Hydrological Processes* **17**: 2855–2869.

Yoshino F. 2002. *Radar Hydrology*. Morikita Shuppan Co., Ltd.

